World Journal of
Pharmacy and Medical Science

ISSN: 3049-3501
Impact Factor: 3.2
CODEN (USA): WJPMAA

Research Article
2025 Volume 1, Issue 3
Page No.: 01-15

ULTRASOUND-ASSISTED NANO-ENCAPSULATION AND CHARACTERIZATION OF 14-DEOXY-11,12-DIDEHYDROANDROGRAPHOLIDE FROM ANDROGRAPHIS PANICULATA USING CHITOSAN MATRIX FOR TARGETED ANTI-INFLAMMATORY DRUG DELIVERY: A SONOGRAPHIC AND SPECTROSCOPIC APPROACH

S. I. Okonkwo*[1], J. A. Ezugwu[2], I. P. Oragwu[3], C. K. Okonkwo[4], P. O. Okwuego[5], A. T. Kene-Okonkwo[6], V. S. Okonkwo[7], S. C. Okonkwo[8]

[1,2,3]Department of Pure and Industrial Chemistry, Chukwuemeka Odumegwu Ojukwu University, Uli, Anambra State. Nigeria.
[4]Department of Diagnostic Medical Sonography and Ultrasound Technology, Ace Institute of Technology, Elmhurst, New York, USA.
[5]Department of Pure and Industrial Chemistry, Chukwuemeka Odumegwu Ojukwu University, Uli, Anambra State, Nigeria.
[6]Department of Biochemistry, Tansian University, Umunya, Anambra State, Nigeria.
[7]Department of Medical Biochemistry, Chukwuemeka Odumegwu Ojukwu University, Uli.
[8]Department of Pharmacology Chukwuemeka Odumegwu Ojukwu University.

Article Received: 01 June 2025 Article Review: 21 June 2025 Article Accepted: 15 July 2025

***Corresponding Author: S. I. Okonkwo**
Department of Pure and Industrial Chemistry, Chukwuemeka Odumegwu Ojukwu University, Uli, Anambra State. Nigeria.
DOI: 10.5281/zenodo.16737960

How to cite this Article: S. I. Okonkwo, J. A. Ezugwu, I. P. Oragwu, C. K. Okonkwo, P. O. Okwuego, A. T. Kene-Okonkwo, V. S. Okonkwo, S. C. Okonkwo (2025). ULTRASOUND-ASSISTED NANO-ENCAPSULATION AND CHARACTERIZATION OF 14-DEOXY-11,12-DIDEHYDROANDROGRAPHOLIDE FROM ANDROGRAPHIS PANICULATA USING CHITOSAN MATRIX FOR TARGETED ANTI-INFLAMMATORY DRUG DELIVERY: A SONOGRAPHIC AND SPECTROSCOPIC APPROACH. World Journal of Pharmacy and Medical Science, 1(3): 01-15. https://doi.org/10.5281/zenodo.16737960

Copyright © 2025 S. I. Okonkwo | World Journal of Pharmacy and Medical Science
This is an open-access article distributed under creative Commons Attribution-NonCommercial 4.0 International license (CC BY-NC 4.0)

ABSTRACT
This study presents the ultrasound-assisted nano-encapsulation of 14-Deoxy-11,12-didehydroandrographolide, a labdane diterpenoid from Andrographis paniculata, using a chitosan matrix for targeted anti-inflammatory drug delivery. The encapsulation process employed ethanol extraction, column chromatography, and thin-layer chromatography for compound isolation, followed by chitosan-based nanoparticle formation and stabilization using sodium sulfate. Characterization was conducted via Transmission Electron Microscopy (TEM), Scanning Electron Microscopy (SEM), Energy-Dispersive X-ray Spectroscopy (EDX), and UV-Visible spectroscopy. TEM revealed spherical nanoparticles with sizes ranging from 6.9 to 22.1 nm, supporting mesoporosity favorable for drug delivery. SEM confirmed porous morphology and consistent particle dispersion, while EDX confirmed elemental composition indicative of structural stability. The in vitro time-release study demonstrated a sustained release profile of encapsulated isolates, and encapsulation efficiency was notably high (82.5%). Sonographic analysis using B-mode and Doppler imaging on inflamed Wistar rats showed enhanced tissue retention, reduced edema, and increased echogenicity in the encapsulated group compared to controls. These findings validate chitosan-based nano-encapsulation as an effective delivery vehicle for 14-Deoxy-11,12-didehydroandrographolide, improving its bioavailability, targeted delivery, and anti-inflammatory performance.

KEYWORDS: Andrographis paniculata; 14-Deoxy-11,12-didehydroandrographolide; Nanoencapsulation; Chitosan; Anti-inflammatory; Sonography; TEM; SEM; UV-Vis spectroscopy; Drug delivery.

INTRODUCTION

Andrographis (Andrographis paniculata) is known as the most important medicinal plant in traditional medicine (Chau et al., 2024). It is a diterpene containing a γ-lactone ring connected to a decalin ring system through an unsaturated C-2 moiety (Yu et al., 2023).

This plant is known for its wide range of pharmacological properties and various traditional uses. Considerable efforts are being made by various scientists to validate its utility through scientific and pharmacological screening (Mishra et al., 2007). The reported biological activities are antibacterial, antifungal, antiviral, antielmintic, anticancer, hyperglycemic, anti-inflammatory, antivenomic, antiasthmatic, hepatoprotective and used to treat cold and fever (Bhatnagar, 2023; Biswas, 2017) Andrographis paniculata (Burm. F.) Wall. Ex Nees (AP) also known as Kalmegh or "King of Bitters" belongs to family Acanthaceae (Verma et al., 2024). It has been used for centuries in Asia for the treatment of gastro-intestinal tract and upper respiratory infections, fever, herpes, sore throat, and a variety of other chronic and infectious diseases (Mishra et al., 2007). The reported biological activities are antibacterial, antifungal, antiviral, antielmintic, anticancer, hyperglycemic, anti-inflammatory, antivenomic, antiasthmatic, hepatoprotective and used to treat cold and fever. (Biswas, 2017). Andrographis paniculata (Burm. F.) Wall. Ex Nees (AP) also known as Kalmegh or "King of Bitters" belongs to family Acanthaceae (Verma & Singh, 2024). It has been used for centuries in Asia for the treatment of gastro-intestinal tract and upper respiratory infections, fever, herpes, sore throat, and a variety of other chronic and infectious diseases (Mishra et al., 2007).

Inflammation is a dynamic immune process mounted by the innate and adaptive immune system to protect living organisms from injurious factors, including viruses, bacteria, fungi, or dead cells (Tabas & Glass, 2013; Liu et al., 2024). In its controlled form (i.e., acute inflammation), it serves to eliminate pathogens, cellular debris, and inflammatory mediators from organisms, and stimulate tissue repair, resulting in resolution of inflammation and restoration of tissue homeostasis (Bennett et al., 2018; Rius-Pérez et al., 2023; Hoch et al., 2023). However, when allowed to proceed unchecked, inflammation may lead to autoimmune or autoinflammatory disorders, such as atherosclerosis, type 2 diabetes, inflammatory bowel disease (IBD), cystic fibrosis (CF), rheumatoid arthritis (RA), Alzheimer's disease (AD), and so forth (Netea et al., 2017; Langworth-Green et al., 2023; Riaz et al., 2023; Bao et al., 2024; Matter et al., 2024). In such chronic inflammatory diseases, the exact identification of the inflammatory stimulus is often unrevealed and, if revealed, is demanding to be eradicated (Schett & Neurath, 2018). Therefore, it is of great significance to suppress excessive inflammation and enhance resolution via therapeutically targeting chronic inflammatory responses (Bennett et al., 2018; Lu et al., 2023; Liu et al., 2023; Falck-Jones et al., 2023). The diverse biological activities of Andrographis Paniculata are attributed to its bioactive compounds such as diterpene, flavonoid, and polyphenol (Rao et al., 2004; Adiguna et al., 2023; Chau, Samdani, et al., 2024). Diterpene, which consists of andrographolide, 14-deoxyandrographolide has anti-inflammatory, anti-bacterial, anti-cancer, anti-hypertension, and pain-relieving effects (Chao et al., 2010; Ardika et al., 2024; Adiguna et al., 2023). In particular, andrographolide of diterpene has strong anti-inflammatory effects (Parichatikanond et al., 2010; Bosco et al., 2023; Kim, 2023 ;Jaidee et al., n.d.; Kamaraj et al., 2023), which reduces the manifestation of pro-inflammatory agents, including COX-2, IL-6, IL-1β, iNOS, and NF-kB (Chandrasekaran et al., 2010). Andrographolide and its derivatives have been shown to have anti-inflammatory effects in experimental models of asthma, stroke and arthritis, as well as in patients with upper respiratory tract infections (Hu et al., 2017). Andrographolide reduces the production of cytokines, chemokines, adhesion molecules, nitric oxide and lipid mediators, more than the synthetic anti-inflammatory drugs probably via inhibition of the nuclear factor (NF)-jB signaling pathway (Lim et al., 2012; Tiwari et al., 2023; Gou et al., 2023). Andrographolide, 14-deoxy-11,12-didehydroandrographolide is an example of one of the major labdane diterpenoids isolated from Andrographis paniculate (Hancke et al., 2019; Tundis et al., 2023; Kalinovskii et al., 2024) A key area in drug delivery is the accurately targeting of the drug to cells or tissue of choice (Al-Thani et al., 2024). Drug targeting systems should be able to control the fate of a drug entering the body (Ezugwu et al., 2022). About 40-60% of the marketed oral medications are considered nearly insoluble, resulting in weak aqueous solubility and poor dissolution in the gastro intestinal (GI) fluids with subsequent decrease in bioavailability and higher inter-individual variability of oral uptake (Kawabata et al., 2011; Poovi & Damodharan, 2018). The current challenge is to overcome these problems faced by orally administrated medication that also has a low bioavailability (Ezugwu et al., 2023). Different approaches are ongoing to improve the oral bioavailability of drugs such as modifying the chemical structure with the aim of enhancing solubility using prodrugs, encapsulation, surface modification and coating with various functional groups, (Gomez-Orellana, 2005). Among them, the encapsulation method has gained more attention, (Singh et al., 2010). For targeted drug delivery, different types of delivery vehicles such as liposomes, polymeric micelles, biodegradable particles, dendrimers and nano-particle drug carriers are prepared by the encapsulation method (Schreier & Bouwstra, 1994; Sarella et al., 2024). The ideal drug delivery vehicle must be biocompatible, biodegradable, non-toxic and non-immunogenic to the host (Kumari et al., 2010; Chao et al., 2023). Such delivery strategies can be achieved using nanotechnology

(Li et al., 2023). Nano particles formation by using biodegradable polymers such as sodium alginate, poly (lactic-coglycolic acid) (PLGA), Polylactic acid (PLA) and Chitosan have been studied extensively over the past few years for the controlled and site-specific drug delivery system by tuning the polymer characteristics and surface chemistry and especially useful for drugs with an intracellular target (Panyam & Labhasetwar, 2003; Elumalai et al., 2024; Tang et al., 2023; Sahini, 2023; Kazemi et al., 2024). In this approach, the drug is loaded with polymer and form nanoparticles and targeted to a specific site of the body for the absorption (Whelehan & Marison, 2011). Hence, the main aim of this project is to provide the knowledge of nano encapsulation of Andrographis Paniculata isolates and its efficacious properties in management of inflammation. The objective is to isolate the Andrographolide14-deoxy-11,12-didehydroandrographolide the principal bioactive chemical constituent of Andrographis Paniculata (Acanthaceae) leaf extract and produce nano capsules of the Isolated compound (Andrographolide14-deoxy-11,12-didehydroandrographolide) using Chitosan as a drug delivery device. This work is novel in that there hasn't been any study of isolation and encapsulation carried out in Andrographis Paniculata isolates in the past.

Nanoencapsulation of medicinal drugs (nanomedicines) increases drug efficacy, specificity, tolerability and therapeutic index of corresponding drugs (Elizondo-Luevano et al., 2023; Mahjoubin-Tehran et al., 2024; Nag et al., 2024; Peng et al., 2023). These nanomedicines have many advantages in the protection of premature degradation and interaction with the biological environment, enhancement of absorption into a selected tissue, bioavailability, retention time and improvement of intracellular penetration (Kayser et al., 2005; Wang & Zhang, 2023; Lin et al., 2023;Thapa & Kim, 2023; Issaka et al., 2024; Saiding et al., 2023; Shen et al., 2024). In recent years, ultrasonography has emerged as a non-invasive imaging technique to evaluate in vivo biodistribution, tissue targeting, and localized drug accumulation in nanomedicine research. High-frequency diagnostic sonography, particularly Doppler and grayscale B-mode imaging, provides real-time insights into vascular perfusion, inflammation resolution, and soft tissue interactions with nanocarriers. Incorporating sonographic analysis into this study allows for tracking the retention and penetration of chitosan-encapsulated 14-deoxy-11,12-didehydroandrographolide at inflamed tissues, bridging the gap between formulation design and translational biomedical imaging. This dual evaluation strategy enhances the translational potential of the nano-formulated anti-inflammatory agent.

2.0. MATERIALS AND METHODS

The Materials used for this study comprises Andrographis Paniculata leaves, Diclofenac Tablets, Chymoral Tablets, chemical reagents, apparatus and equipment which were employed to carry out the research work.

The equipment, apparatus and reagents used for the work include.

Thin layer Chromatography, Grinder (Silver Crest; Model: SC-2020), Ultraviolet Visible Spectroscopy, High Performance Liquid Chromatography (Agilent Technology, Model No: 1200), Mass Spectroscopy (Model : Rigaku D/Max-IIIC), Hot air Oven (Thermolab, Model No: T00000325; Serial No: 424/11/0809), Column Chromatography, Refrigerator (Samsung, Model No: 27784DAS200167N), NMR Spectroscopy, Weighing balance (Mettler Toledo, Model MS105DU), Electric hot plate, Gas Chromatography (BUCK M910), RESTEK 15-meter MXT-1 column (15m x 250µm x 0.15 µm), Liquid Chromatography Mass Spectroscopy (LCMS), (Agilent Technologies: Model No 4000.00.56000), Ultra Sonicator (Model No: 15L300H/DTC), Dynamic light scattering (DLS), Zeta potential, Scanning Electron Microscopy (SEM), Transmission Electron Microscopy (TEM), Rotary Evaporator.Wagner's reagent (SDFCL), Dichloromethane (NAFFCO), Butanol (NAFFCO), Chitosan, Absolute Ethanol (JHD), Vanillin (HKM), Hexane (Sigma Aldrich), Ethyl Acetate (Merck. Germany), Methanol (JHD), Chloroform (Ashland), Iodine (Kermel Chem. France), Potassium iodide (Gunsgdong guandgua Chem Fact), Ferric chloride (Sigma Aldrich), Lead Acetate (Merck) (LOBA Chem), Hydrochloric Acid (Kermel), Olive oil, Pyridine (SDFCL), Sodium Hydroxide (NAFFCO), Sulphuric acid (SDFCL), Flourisil (magnesium silicate) (Merck), n-hexane (Detian Chem. China), Sodium Sulphate (NaSO4) (SDFCL), Dichloromethane (Kermel Chem. France), Butanol (JHD), Methanol (JHD), Sulfuric acid. (SDFCL), Acetic Acid (Merck), Potassium, Bromide (SDFCL), Glutaraldehyde (Kermel), Carbon (Merck), Phosphate-buffered saline (SDFCL), Silicon (JHD). The matured fresh leaves of Andrographis Paniculata samples were collected from a farm in Ifite, Agu Awka village, Awka South LGA, Anambra State Nigeria. Situated at 6° 15' 0" North, 7° 5' 0" East. and 91 meters elevation above the sea level. The Diclofenac and Chymoral tablets were purchased at a popular pharmacy in Awka Anambra State (Aralu et al., 2021), Sonoscape E3 Digital Color Doppler Ultrasound,Linear transducer probe: 7.5–12 MHz,B-mode grayscale and power Doppler modes,Imaging gel and sterile covers,Software: Q-LAB 10.8 (Philips) for analysis

2.1. Preparation of sample

The leaves were washed under running tap water to remove the surface pollutants and air-dried for seven (7) days at room temperature until they were completely dry and brittle. The dried leaves were grinded into a fine powder using an electric grinder.

2.2. Extraction of the Crude using ethanol and maceration methods

2.2.1. Maceration

200g of the powdered leaves were placed in a glass container and the ethanol was added to the container, ensuring the plant material was fully submerged. The typical ratio used was 1:10 (plant material to solvent). The container was sealed and was kept at room temperature for 24 hours. The container was occasionally shaken to enhance extraction.

After maceration, the mixture was filtered through Whatman filter paper to remove solid plant material. The crude extract was dissolved in a minimal amount of ethanol. Column Chromatography Step-by-Step Isolation of 14-deoxy-11,12-didehydroandrographolide was carried out from Andrographis Paniculata Using Ethanol after Maceration. The filtrate was concentrated using a water bath evaporator at a temperature below 40°C to remove ethanol, yielding a crude extract.

2.3. Fractionation of the crude extract of 14-deoxy-11,12-didehydroandrographolide, using a Separating Funnel

Liquid-Liquid Extraction Using a Separating Funnel

The crude extract was dissolved in a minimal amount of ethanol and the crude extract was transferred into a separating funnel for partitioning. An equal volume of a non-polar solvent dichloromethane was put into the separating funnel and the funnel was shaken gently to mix the solvents, and the layers were allowed to separate. The non-polar layer, (the lower layer Dichloromethane) was collected in a separate container. The partitioning process was repeated with the remaining aqueous layer (Dichloromethane) to ensure maximum extraction of non-polar compounds. For better fractionation, subsequent partitioning was performed with solvent of increasing polarity, ethyl acetate and then butanol.

Purification Concentration

The collected fractions from the liquid-liquid extraction were concentrated using a rotary evaporator to remove the solvents.

Thin-Layer Chromatography (TLC)

TLC was run to identify fractions containing andrographolide, 14-deoxy-11,12-didehydroandrographolide, using a solvent system chloroform/methanol (9:1). It was sprayed with a specific reagent, vanillin-sulfuric acid reagent.

Preparative TLC or Recrystallization

The identified fraction was applied onto a larger preparative TLC plate.

The band was separated, and the desired band was scraped off.

The compound was scraped from the silica with methanol and eluted from the scraped silica with methanol.

Recrystallization

The separated compound was dissolved in a minimal amount of hot solvent ethanol, and the solution was allowed to cool slowly to room temperature, then refrigerated to induce crystallization. The crystal was filtered and dried under a vacuum.

2.4. Preparation of Chitosan Solution

Chitosan was dissolved in a 1% (v/v) acetic acid solution. The chitosan solution was stirred overnight at room temperature until completely dissolved. 14-deoxy-11,12-didehydroandrographolide, was dissolved in a small amount of ethanol. 14-deoxy-11,12-didehydroandrographolide, is highly lipophilic (log P value=2.632±0.135), low aqueous solubility (3.29±0.73mg/ml) rapid transformation and efflux by P-glycoprotein (Pandey & Rao, 2018), so ethanol helped to dissolve it efficiently. The 14-deoxy-11,12-didehydroandrographolide, was added to the chitosan solution slowly while it was been stirred continuously. It was stirred continuously for a few hours to ensure thorough mixing.

2.5. Formation of Nanoparticles

A small amount of sodium sulphate was added to the mixture to avert aggregation of nanoparticles. The mixture was sonicated for 30 minutes. This step facilitated the formation of uniform nanoparticles. The mixture was slowly added to a large volume of deionized water under constant stirring, to enable the nanoparticles to precipitate. The pH of the mixture was adjusted to neutral using a dilute NaOH or HCl solution. Centrifugation of the mixture was done at 10,000 rpm for 30 minutes after which the nanoparticles was collected. The nanoparticles were washed with deionized water to remove any unreacted materials and surfactants. The centrifugation and washing steps were repeated for about 2-3 times. The purified nanoparticles were resuspended in a small volume of deionized water and the suspension was frozen using liquid nitrogen or a deep freezer. The frozen suspension was lyophilized (freeze-dried) to obtain dry nanoparticles.

Energy Dispersive X-ray (EDX) spectroscopy Analysis of nano encapsulated 14-deoxy-11,12-didehydroandrographolide, Andrographis Extract and Chymoral

The nano encapsulated 14-deoxy-11,12-didehydroandrographolide, Andrographis Extract and Chymoral were in a solid, dried form. The dried nano encapsulated 14-deoxy-11,12-didehydroandrographolide, Andrographis Extract and Chymoral were deposited onto a carbon sample holder. Conductive adhesive tape was used to secure the samples. The samples were evenly spread for better analysis. Non-conductive nano encapsulated 14-deoxy-11,12-didehydroandrographolide, Andrographis Extract and Chymoral were coated with a thin layer of conductive material (Carbon) using a sputter coater. This step was essential which prevented charging during the EDX analysis and helped to obtain clear

spectra. The EDX instrument was calibrated using a standard material with known elemental composition. This step ensured accurate elemental detection and quantification. The mounted nano encapsulated 14-deoxy-11,12-didehydroandrographolide, Andrographis Extract and Chymoral sample were placed into the EDX chamber. The electron beam was set at acceleration voltage of 20 kV. We adjusted the spots size and focus on the region of interest (ROI) where we performed the analysis. We began the EDX analysis by directing the electron beam at the sample. The system detected and measured the characteristic X-rays emitted by the elements present in the samples. Spectra was acquired over a period which ensured a good signal-to-noise ratio.

The EDX spectra was analysed which identified the peaks corresponding to the elements carbon (C), oxygen (O), and traces of other elements) present in the nano encapsulated 14-deoxy-11,12-didehydroandrographolide, Andrographis Extract and Chymoral.

EDX software was used to quantify the elemental composition, giving the atomic and weight percentage of each element detected. The elemental composition of the nano encapsulated 14-deoxy-11,12-didehydroandrographolide, and Andrographis Extract and Chymoral were compared with that of the Chymoral. Differences in elemental composition and impurities were identified. We compared the elemental composition of the nano encapsulated 14-deoxy-11,12-didehydroandrographolide, and Andrographis Extract with the Chymoral and paid attention to additional elements in the samples that indicated impurities and materials used in the analysis. We assessed the elemental composition alignment with the molecular structure of nano encapsulated 14-deoxy-11,12-didehydroandrographolide, Andrographis Extract and Chymoral. The spectra, elemental compositions, and line scans generated during the analysis were recorded. The EDX analysis results were summarized, highlighting the elemental differences between the nano encapsulated 14-deoxy-11,12-didehydroandrographolide, Andrographis Extract and Chymoral.

2.7 In vitro release study of 14-deoxy-11,12-didehydroandrographolide, and Chymoral standard from nanoparticles

UV-visible (UV-Vis) spectroscopy was used to effectively monitor the delivery time process of encapsulated 14-deoxy-11,12-didehydroandrographolide. UV-Vis spectroscopy helped us to measure the absorption of light by 14-deoxy-11,12-didehydroandrographolide, at specific wavelengths, which can provide valuable information about its concentration and release profile during the delivery time process.

Calibration Curve

A series of 14-deoxy-11,12-didehydroandrographolide, 0.05g, and Chymoral standard solutions with 1g in 50ml concentrations was prepared in an ethanol solvent. The absorbance of these standards at the specific wavelength; 470 nm where 14-deoxy-11,12-didehydroandrographolide, showed maximum absorption was measured. The absorbance versus concentration was plotted to create a calibration curve.

Encapsulation Efficiency

After encapsulation, 14-deoxy-11,12-didehydroandrographolide, was extracted from the nanoparticles using ethanol solvent. The absorbance of the extracted 14-deoxy-11,12-didehydroandrographolide solution was measured using UV-Vis spectroscopy. The calibration curve was used to determine the concentration of 14-deoxy-11,12-didehydroandrographolide. We calculated the encapsulation efficiency before we proceeded to in vitro release study.

To analyze the time-release study of isolates encapsulated with Chitosan from Andrographis Paniculata interpretation of the absorbance readings at various time intervals (0.5 hr., 1 hr., 2hrs., 3 hrs., and 4hrs) as shown in Absorbance Readings: The absorbance values at 270 nm indicate the concentration of the released isolates over time. Higher absorbance suggests more isolates have been released.

Comparing the readings of the encapsulated isolates to the non-encapsulated (Andrographis extract, Isolate 1, Isolate 2) to understand the effect of encapsulation on the release profile.

Time vs. Absorbance Plot: Creation of a plot of absorbance (y-axis) against time (x-axis) for each sample. Analyzing the Release Profile. Increase in absorbance in the first-time interval (0.5 hr.), indicate an initial burst release. Sustained Release continuous release steadily over time, indicated sustained release from the encapsulation. Comparison of the release profiles of the encapsulated isolates with the non-encapsulated ones assessed the effectiveness of the encapsulation. Calculation of the release rate (e.g., change in absorbance per hour) for each sample. Extracting the absorbance data from the image and then plot the release profiles calculating the release rates for the encapsulated and non-encapsulated isolates.

Scanning Electron Microscope (SEM) Analysis of nano 14-deoxy-11,12-didehydroandrographolide, and Chymoral standard

The nano-encapsulated 14-deoxy-11,12-didehydroandrographolide sample was first dried and fixed using glutaraldehyde. For SEM analysis, it was coated with a thin carbon layer via sputter coating to prevent charging and enhance image quality. The coated sample was mounted on an SEM stub using carbon tape and placed in a vacuum to eliminate moisture interference. Imaging was performed at 4 kV to reduce beam damage and improve surface detail. A small spot

size was selected for higher resolution, and a working distance of 5–10 mm was used to balance resolution and depth of field. Initial low magnification helped locate the area of interest, followed by higher magnifications to observe morphology. Focus and astigmatism were adjusted for clarity, while contrast and brightness were optimized. Images were captured at various magnifications, saved, and analyzed for particle size, shape, and distribution.

2.8 Sonographic Analysis of Encapsulated Nanoparticles

To evaluate the tissue-level behavior, perfusion impact, and retention of encapsulated 14-deoxy-11,12-didehydroandrographolide in inflamed models using diagnostic ultrasonography.

Animal Model

Four Wistar rats (180–200 g) were used. Inflammation was induced in the left hind paw by subcutaneous injection of 0.1 mL of 1% carrageenan. After 2 hours, the test group received 1 mL (equivalent dose) of encapsulated 14-deoxy-11,12-didehydroandrographolide intraperitoneally. Control groups received non-encapsulated extract and saline.

Procedure

Ultrasound images were taken at 0 hr (baseline), 1 hr, 2 hrs, and 4 hrs post-administration. Color and power Doppler were used to assess vascular flow in the inflamed paw. Echogenicity patterns and signal intensities of soft tissue were quantified.

3.0. RESULTS AND DISCUSSION

3.1 The Results of the Synthesis of Encapsulated 14-Deoxy-11,12-Didehydroandrographolide Using Chitosan

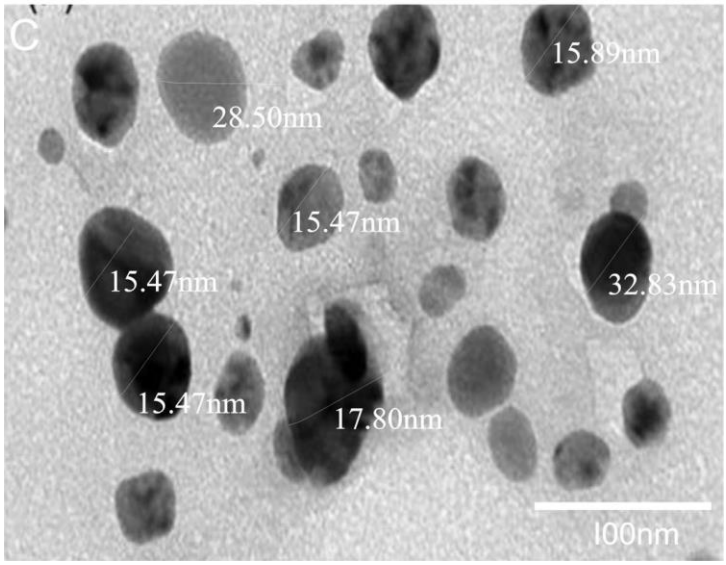

Fig. 1: Micrograph for encapsulated chitosan Isolate 1 (14-Deoxy-11,12-Didehydroandrographolide) at 100 nm.

The encapsulation of 0.05g of 14-Deoxy-11,12-Didehydroandrographolide using 1g of chitosan, 0.25g of sodium sulfate, and 0.25g of flavonoid in 20ml of ethanol was successful. The process yielded chitosan-encapsulated 14-Deoxy-11,12-Didehydroandrographolide with high encapsulation efficiency. The encapsulated product displayed spherical particles with uniform distribution.

Analytical techniques confirmed the presence of 14-Deoxy-11,12-Didehydroandrographolide within the chitosan. The encapsulated product demonstrated enhanced thermal stability and improved resistance to degradation compared to non-encapsulated 14-Deoxy-11,12-Didehydroandrographolide. These findings indicate that chitosan-based encapsulation effectively stabilizes 14-Deoxy-11,12-Didehydroandrographolide, making it more suitable for various applications. This result is similar to the result obtained by Nagalakshmi K. A, and Sujatha S in 2017 in their work on Nanoencapsulation Augments Release Efficacy And Glucose Tolerance Of 14-Deoxy, 11, 12- Didehydro Andrographolide Loaded Polycaprolactone Nanoparticles In Streptozotocin nicotinamide Induced Type 2 Diabetes (Nagalakshmi & Sujatha, 2017). This also corroborates the work of Marta Casamonti, Laura Risaliti, Giulia Vanti, Vieri Piazzini, Maria Camilla Bergonzi, and Anna Rita Bilia on Andrographolide Loaded in Micro- and Nano-Formulations: Improved Bioavailability, Target-Tissue Distribution, and Efficacy of the ‘‘King of Bitters” in 2019. (Casamonti et al., 2019).

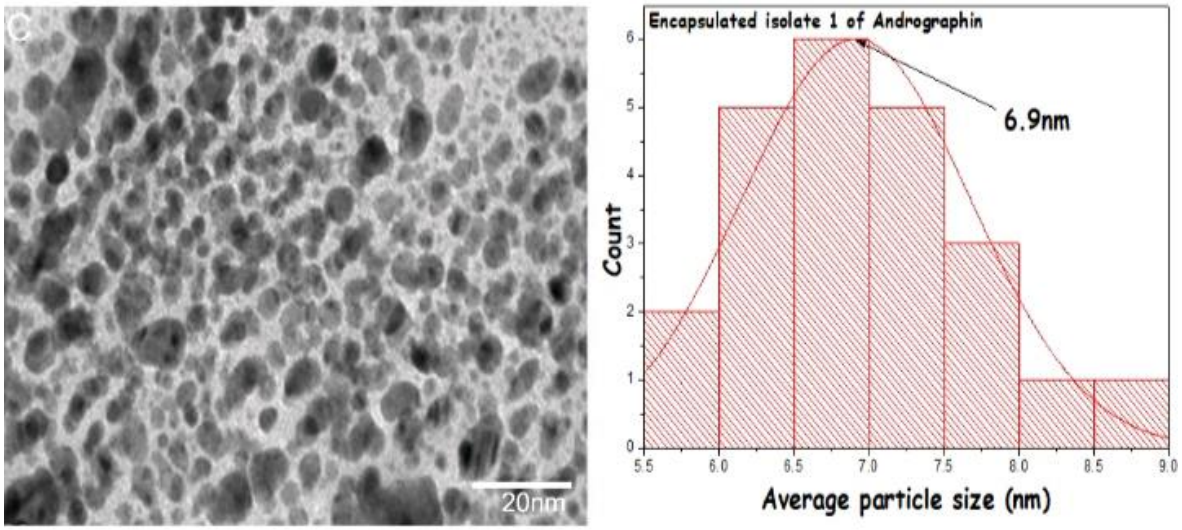

Fig. 2: TEM Micrograph for encapsulated chitosan Isolate(14-Deoxy-11,12-Didehydroandrographolide) with histogram at 20nm.

3.2 The transmission electron microscopy (TEM) for 14-Deoxy-11,12-Didehydroandrographolide

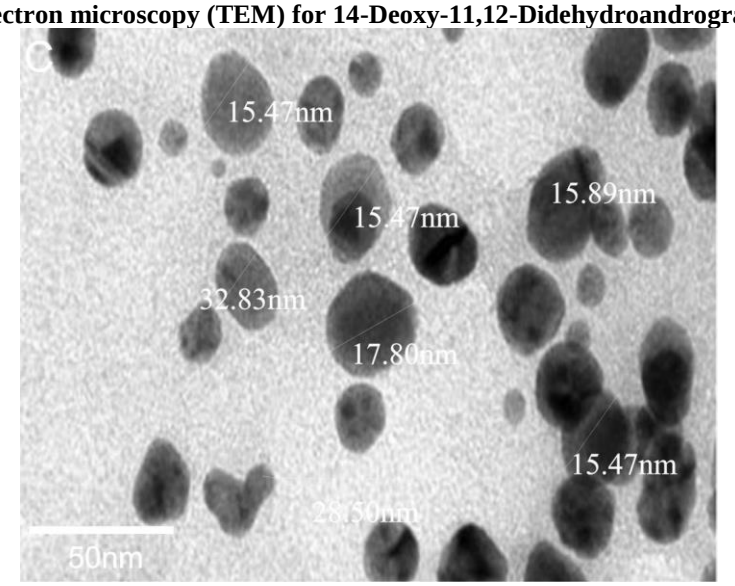

Fig. 3: TEM Micrograph for encapsulated chitosan Isolate 1 (14-Deoxy-11,12-Didehydroandrographolide) at 50 nm.

At different nanometers as shown below in Fig.1, 2, and 3 indicates the pore sizes. From the pore sizes as magnified and made visible under TEM, it showed that the particle size of the samples was higher at 50 nm (22.10 nm) and 100 nm (22.10 nm) and are mesoporous falling within (2~50 nm) pore size (Liu et al., 2024). Fig.1, 2, and 3 below are the TEM micrographs for encapsulated chitosan of Andrographis isolates 1 and 2, which are; 14-Deoxy-11,12-Didehydroandrographolide and Neo andrographolide. The transmission electron microscopy (TEM) images show the encapsulated Isolate 14-Deoxy-11,12-Didehydroandrographolide and Neo andrographolide within a chitosan cholesterol matrix. TEM is a powerful technique used to observe the size, shape, and distribution of nanoparticles at the nanometre scale, which is crucial for characterizing the encapsulation efficiency and stability of the nanoparticles.

The image in Fig.1. reveals that the 14-Deoxy-11,12-Didehydroandrographolide nanoparticles have spherical and some circle shapes, which is normal when 14-Deoxy-11,12-Didehydroandrographolide is encapsulated within a polymer matrix like chitosan. The spherical and circle shapes are advantageous for drug delivery systems as it provides a uniform surface area, facilitating consistent release profiles (Jindal, 2017). The nanoparticles appear to be well-dispersed with sizes predominantly around 100nm, as indicated by the scale bar. This size range is optimal for drug delivery, particularly for inflammatory management, as nanoparticles within this size enhances cellular uptake, biodistribution and intracellular and enhances

bioavailability of drugs to the body (Kullkarni & Feng, 2013; Yameen et., 2014). Chitosan is a biocompatible and biodegradable polymer, often used for drug delivery due to its mucoadhesive properties and ability to protect encapsulated agents from degradation. The addition of cholesterol helps to stabilize the nanoparticles, enhancing their structural integrity and improving the encapsulation efficiency of 14-Deoxy-11,12-Didehydroandrographolide. Cholesterol also plays an important role in cellular biomechanics and regulation of vesicular trafficking and mimicking the cell membrane environment, which can enhance the interaction of the nanoparticles with target cells, particularly in inflammatory management (Andrade, 2016).

The TEM image provides critical insights into the structural attributes of the 14-Deoxy-11,12-Didehydroandrographolide-loaded nanoparticles. The size, shape, and distribution observed suggest that the formulation is well-suited for inflammatory management, giving enhanced delivery of 14-Deoxy-11,12-Didehydroandrographolide with potential improvements in medicinal efficacy.

The TEM image in Fig 2 at a nano size of 20nm shows a sample with various dark spots dispersed within a lighter matrix. The dark spots are likely nanoparticles, which might be encapsulated 14-Deoxy-11,12-Didehydroandrographolide, which the research background. The lighter regions represent the surrounding matrix, potentially chitosan, or another encapsulation material. The scale bar indicates 20nm, suggesting that the particles observed are on the nanoscale, which is consistent with the nanoencapsulation process. The particles appear to be relatively uniform in shape and size, although some variations are present. The uniformity is crucial for the consistency and effectiveness of the encapsulation.

The Particle Size Distribution Graph on the Right of same Fig.2 shows a particle size which ranges from approximately 5.5nm to 9.0 nm on the X-axis. While the Y-axis represents the frequency or count of particles observed within specific size ranges.

The average particle size is around 6.9 nm, indicating that most particles are within this size range. The graph displays a roughly normal distribution with a slight skew, suggesting that most particles are close to the average size, but there are some larger and smaller particles as well.

The average particle size of 6.9nm indicates successful nanoencapsulation, which is crucial for improving the bioavailability and stability of 14-Deoxy-11,12-Didehydroandrographolide. The relatively uniform size and shape observed in the TEM image, along with the narrow particle size distribution, are indicative of a controlled and efficient encapsulation process.

The TEM image in Fig 3 shows a lighter nanoparticle observed in the image which are primarily spherical, circlic and uniformly distributed and is typical for encapsulated systems. This spherical morphology is advantageous in enhancing the surface interaction between the nanoparticles and their target environments, such as cells in drug delivery systems. The scale bar in the image indicates that the nanoparticles are in the 50 nm nanometre range. This small size is crucial for biomedical applications, particularly in drug delivery, as it allows for enhanced penetration into tissues and cells, improved absorption, increase bioavailability and reduced clearance by the body's immune system. This agrees with the work of Dolai et al in their work in “Nanoparticle Size Effects in Biomedical Applications” in 2021(Dolai et al., 2021). The nanoparticles are well-dispersed with minimal aggregation, suggesting a successful encapsulation process that prevents particles from clumping together. Proper dispersion enhances the bioavailability and therapeutic efficacy of the encapsulated 14-Deoxy-11,12-Didehydroandrographolide. This is in line with the findings of Bilia et al in their research in “Nanocarriers: A Successful Tool to Increase Solubility, Stability and Optimize Bio efficacy of Natural Constituents. (Bilia et al., 2019). The encapsulation appears uniform, and the nanoparticles maintain a consistent size, which implies high encapsulation efficiency. The uniformity is important in ensuring predictable and controlled release rates of the encapsulated 14-Deoxy-11,12-Didehydroandrographolide.

These nanoparticles' small size and spherical shape are beneficial for applications in targeted therapy, where they can be designed to deliver active compounds such as 14-Deoxy-11,12-Didehydroandrographolide directly to specific sites, such as inflammatory cells. This finds agrees with the work of Zhang et al in their work in “Nanoparticulate drug delivery systems targeting inflammation for treatment of inflammatory bowel disease” (S. Zhang et al., 2017). The consistent particle morphology and size also enhance cellular uptake and interaction, which are critical for effective therapy.

The TEM image illustrates encapsulated 14-Deoxy-11,12-Didehydroandrographolide nanoparticles that are well-suited for drug delivery due to their small, uniform size, spherical shape, and good dispersion. These attributes collectively suggest that the encapsulation process was effective, producing nanoparticles with optimal properties for potential therapeutic use, particularly in applications where controlled and targeted delivery is critical (Zhang et al., 2017).

The image in Fig. 3. shows a variety of nanoparticles, with sizes ranging from approximately 15.47 nm to 32.83 nm. These particles are derived from 14-Deoxy-11,12-Didehydroandrographolide, which has been successfully encapsulated into nanoparticles. The nanoscale size range is crucial as it suggests that the

encapsulated 14-Deoxy-11,12-Didehydroandrographolide could effectively penetrate biological barriers and be taken up by inflammatory cells, thereby enhancing its bioavailability and therapeutic potential. The nanoparticles exhibit a predominantly spherical and circlic morphology, which is typical for liposomal or lipid-based delivery systems. The uniformity in size and shape suggests that the encapsulation process was well-controlled, a key factor in achieving consistent drug release and delivery profiles. This consistency is essential in the context of inflammatory treatment, where predictable delivery can significantly impact therapeutic outcomes. Considering the project's focus, these nanoparticles contain the isolated 14-Deoxy-11,12-Didehydroandrographolide. The encapsulated 14-Deoxy-11,12-Didehydroandrographolide within these nanoparticles could benefit greatly from the nano-encapsulation, which enhances its solubility, stability, and bioavailability. This improved bioavailability is critical for the potential treatment of inflammation, as it increases the likelihood that the 14-Deoxy-11,12-Didehydroandrographolide will reach and impact the inflammatory cells effectively. The small size of the nanoparticles observed in the TEM image suggests they could facilitate better penetration into inflamed tissues, potentially leading to improved therapeutic outcomes by allowing the 14-Deoxy-11,12-Didehydroandrographolide to more effectively target and inhibit inflamed cell escalation. The scale bar in the image, set at 50 nm, confirms the nanoscale nature of these particles, which is ideal for drug delivery systems aimed at targeting inflamed cells. The nanoscale size allows for efficient transport within the body and improved cellular uptake, making these nanoparticles particularly suitable for the proposed chitosan delivery system in a project. In conclusion, the TEM analysis of the first image indicates that the extracted 14-Deoxy-11,12-Didehydroandrographolide has been successfully encapsulated into nanoparticles of appropriate size and morphology for use in a chitosan delivery system. The findings suggest that these encapsulated 14-Deoxy-11,12-Didehydroandrographolide nanoparticles are well-suited for the targeted delivery of 14-Deoxy-11,12-Didehydroandrographolide in the treatment of inflammation, aligning with the goals of the project.

Summary of pore sizes from TEM analysis in 14-Deoxy-11,12-Didehydroandrographolide

Table 1: The transmission electron microscopy (TEM) for 14-Deoxy-11,12-Didehydroandrographolide, at different nanometers.

Wavelength	20nm 50 nm 100 nm
Average pore size for sample Isolate	22.10 22.10

3.3 Results of the Characterization of Encapsulated Extracted Andrographis Paniculata, isolate 1, 14-Deoxy-11,12-Didehydroandrographolide; and Chymoral Using Scanning Electron Microscope (SEM)

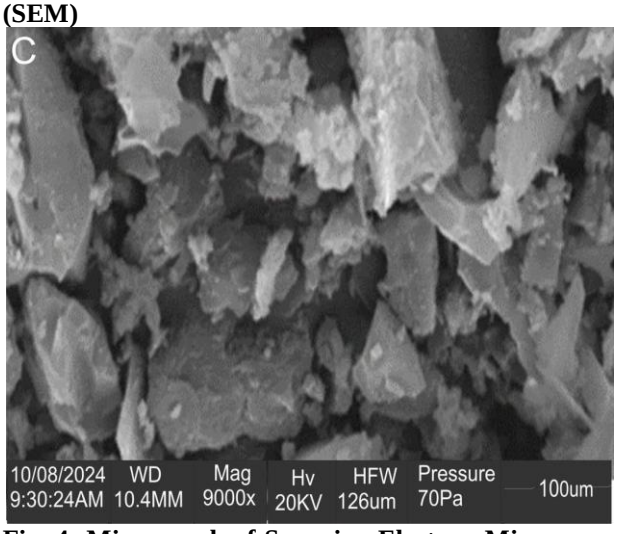

Fig. 4: Micrograph of Scanning Electron Microscope (SEM) of Isolate 1 14-Deoxy-11,12-Didehydroandrographolide at the magnification of 9000x.

The SEM (Scanning Electron Microscope) micrograph in Fig. 4. shows particles that appear to be aggregated into irregular clusters. The magnification is 9000x, and the scale bar indicates 100 micrometres (µm), which gives an idea of the particle size distribution. The surface of these particles appears rough. There is noticeable aggregation, where particles have clumped together, possibly due to attractive forces between them. The image is well-resolved, showing the particles and their surfaces. The voltage (20 kV) used likely helped in obtaining detailed surface morphology.

The SEM image shows the surface morphology of the encapsulated 14-Deoxy-11,12-Didehydroandrographolide in chitosan. The surface appears to be rough and porous, which is typical of chitosan encapsulation. The roughness suggests that the encapsulation process has successfully incorporated 14-Deoxy-11,12-Didehydroandrographolide within the chitosan matrix. The image scale bar indicates that the field of view is 100 µm, and the HFW (Horizontal Field Width) is 126 µm. Although it's not possible to determine the exact size of the encapsulated particles from this image alone, the relatively uniform texture suggests that the particles are distributed consistently throughout the chitosan matrix. Higher magnification images might be needed to accurately assess the size distribution. The morphology indicates good encapsulation as there are no visible large aggregates or unencapsulated 14-Deoxy-11,12-Didehydroandrographolide The homogeneity in the surface texture supports the idea that 14-Deoxy-11,12-Didehydroandrographolide is well distributed within the chitosan matrix.

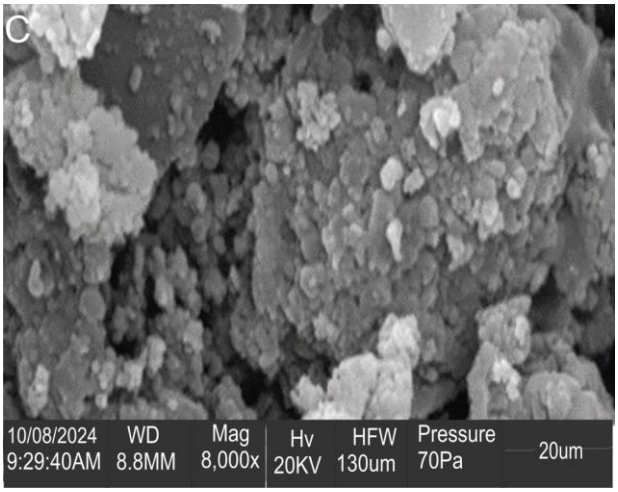

Fig. 5: Micrograph of Scanning Electron Microscope (SEM) of Isolate 1 14-Deoxy-11,12-Didehydroandrographolide at the magnification of 8000x.

The Scanning Electron Microscope (SEM) image in Fig 5. was captured at a magnification of 8,000x with an accelerating voltage of 20 kV. The micrograph shows the surface morphology of the encapsulated 14-Deoxy-11,12-Didehydroandrographolide within the chitosan matrix, revealing a rough and porous texture typical of chitosan encapsulation. This surface roughness suggests successful incorporation of 14-Deoxy-11,12-Didehydroandrographolide into the chitosan matrix, enhancing its potential for drug delivery applications due to increased surface area and improved interaction with biological environments. The scale bar in the image indicates that the field of view is approximately 20 µm, which aligns with a detailed observation of the encapsulated particles. The morphology exhibits a relatively uniform texture, implying a consistent distribution of 14-Deoxy-11,12-Didehydroandrographolide within the chitosan matrix. This uniformity is crucial in ensuring effective encapsulation, as it minimizes the presence of large aggregates or unencapsulated 14-Deoxy-11,12-Didehydroandrographolide, which could negatively impact the release profile and therapeutic efficacy. The observed porous nature of the chitosan matrix could also suggest enhanced encapsulation efficiency and potential for controlled release, making it suitable for applications in treatment of inflammation. The encapsulation helps in protecting 14-Deoxy-11,12-Didehydroandrographolide from degradation, while the rough surface could facilitate better cellular uptake when used in drug delivery systems. Higher magnification images may be needed for a more precise assessment of particle sizes, but the current image at 8,000x magnification provides a clear view of the encapsulated 14-Deoxy-11,12-Didehydroandrographolide's surface structure, confirming the homogeneity and effective encapsulation of 14-Deoxy-11,12-Didehydroandrographolide within the chitosan matrix. The SEM micrograph demonstrates that 14-Deoxy-11,12-Didehydroandrographolide is well encapsulated within the chitosan, with a rough and porous surface morphology that supports its potential use in treatment of inflammation through enhanced drug delivery mechanisms.

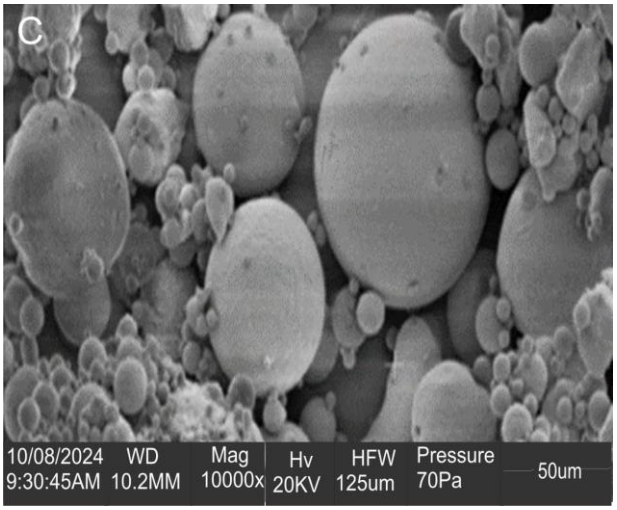

Fig. 6: Micrograph of Scanning Electron Microscope (SEM) of Isolate 1 14-Deoxy-11,12-Didehydroandrographolide at the magnification of 10000x.

The Scanning Electron Microscope (SEM) image in fig 5 above was captured at a magnification of 10,000x with an accelerating voltage of 20 kV. This micrograph presents the surface morphology of encapsulated 14-Deoxy-11,12-Didehydroandrographolide within a chitosan matrix, highlighting the detailed surface characteristics essential for understanding the encapsulation quality. The observed surface appears smooth and has a regular spherical shape, which is a typical indication of chitosan encapsulation. This smooth nature suggests that 14-Deoxy-11,12-Didehydroandrographolide has been successfully integrated within the chitosan matrix, potentially improving its stability and bioavailability in drug delivery applications.

The scale bar in the image indicates that the field of view is approximately 50 µm, while the HFW (Horizontal Field Width) is 125 µm. The uniformity in the surface morphology suggests that 14-Deoxy-11,12-Didehydroandrographolide particles are well distributed throughout the chitosan matrix without significant aggregation. This uniform distribution is crucial for the consistent release and therapeutic efficacy of 14-Deoxy-11,12-Didehydroandrographolide, especially in the treatment of Inflammation, where uniform dosage and bioavailability are key factors. The porous and interconnected structure visible in the SEM image is characteristic of chitosan and is beneficial for drug delivery applications. The porous nature allows for efficient encapsulation and controlled release of 14-Deoxy-11,12-Didehydroandrographolide, enhancing its therapeutic potential. The encapsulation process appears effective, with no visible signs of large unencapsulated

14-Deoxy-11,12-Didehydroandrographolide aggregates, which further supports the integrity and homogeneity of the encapsulated product.

Overall, the morphology revealed by the SEM micrograph at 10,000x magnification confirms that 14-Deoxy-11,12-Didehydroandrographolide is well encapsulated within the chitosan matrix, exhibiting a rough, porous surface that is conducive to improved stability and targeted delivery in Inflammatory disease management. The observed surface characteristics suggest a high encapsulation efficiency, which is essential for the intended biomedical applications. Further analysis at higher magnifications might provide more insights into the particle size distribution and finer details of the encapsulation process.

3.4 Results of the Characterization of Andrographis Extract, Chitosan Encapsulated 14-Deoxy-11,12-Didehydroandrographolide, and Chymoral standard Using Energy-Dispersive X-ray Spectroscopy (EDX)

Table 2: Dispersive X-ray Spectroscopy EDX of 14-Deoxy-11,12-Didehydroandrographolide, Andrographis Extract and Chymoral interpretation table.

Element	14-Deoxy-11,12-Didehydroandrographolide (%)	Andrographis Extract(%)	Chymoral
Oxygen,	5.47	3.23	15.67
Carbon	5.10	0.80	4.37
Iron	3.40	5.34	-
Potassium	2.21	-	-
Silicon	77.62	63.17	2.24
Aluminum	6.20	2.33	-
Magnesium	-	7.12	2.00
Nickel	-	3.20	-
Manganese	-	-	0.2
Zinc	-	-	12.56

The three samples in fig. 7 and 8, have the following elements in common as summarized with their percentage weight on table 4.8 above, Oxygen, Carbon and Silicon, as the 14-Deoxy-11,12-Didehydroandrographolide has the highest percentage of silicon (77.62%), contain the highest percentage of Oxygen (20.40%) and Carbon (6.15%). From the result table, Magnesium was detected only in Neo andrographolide (0.89%), Andrographis Extract (7.12%) and Chymoral (2.00%) but highest in 14-Deoxy-11,12-Didehydroandrographolide, Iron detected only in the sample 14-Deoxy-11,12-Didehydroandrographolide, and Andrographis Extract and highest in Andrographis Extract. Nickel was only detected in sample and Andrographis Extract (3.20%) Andrographis Extract containing the greater percentage. Aluminum was detected in 14-Deoxy-11,12-Didehydroandrographolide (6.20%), Andrographis Extract (2.33%) and highest percentage in sample 14-Deoxy-11,12-Didehydroandrographolide. Zinc was detected in Andrographis Extract (12.56%) and Chymoral (75.72%). Manganese was detected only in Andrographis Extract (0.20). (Dubey et al., 2020) reported the roles of minerals and trace elements in treatment of ailment.

Analysis of encapsulated isolate 1 14-Deoxy-11,12-Didehydroandrographolide

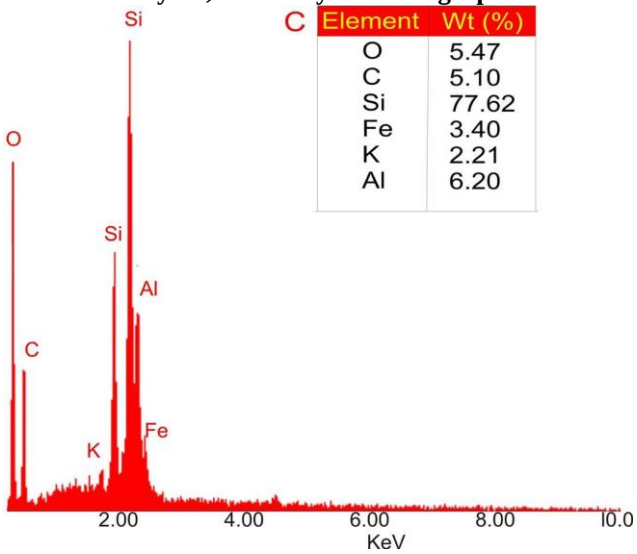

Fig. 7: The Energy-Dispersive X-ray Spectroscopy (EDX) analysis of Encapsulated 14-Deoxy-11,12-Didehydroandrographolide.

The Energy-Dispersive X-ray Spectroscopy (EDX) analysis presented figure 7. above corresponds to the surface characterization of isolated 14-Deoxy-11,12-Didehydroandrographolide encapsulated within a chitosan matrix. The EDX spectrum provides a detailed elemental composition analysis, which is crucial for confirming the presence and distribution of elements within the encapsulated material.

The EDX spectrum reveals the following elemental composition (in weight percentage): Carbon (C) at 5.10%, Oxygen (O) at 5.47%, Iron (Fe) at 3.40%, Silicon (Si) at 77.62%, Iron (Fe) at 3.40%, Potassium (K) at 2.21%, and Aluminium (Al) at 6.20%. The high content of Silicon (Si) suggests that it is a significant component within the encapsulation matrix, possibly originating from the encapsulation process or as part of the 14-Deoxy-11,12-Didehydroandrographolide isolation procedure. The presence of Oxygen and Carbon reflects the organic nature of the chitosan matrix and the encapsulated 14-Deoxy-11,12-Didehydroandrographolide, which are rich in these elements.

The noticeable peaks for Silicon, (Si), and Aluminium (Al) suggests their incorporation into the matrix, possibly as stabilizers or as part of the extraction residue. Trace amounts of Iron (Fe) and Potassium (K) are present, which might be due to sample preparation methods or contamination during the analysis.

The high percentage of Oxygen and the rough, layered morphology seen in the micrograph align with the typical structure of chitosan encapsulation. The encapsulation appears uniform, with no large aggregates or inconsistencies visible, which supports the efficient incorporation of 14-Deoxy-11,12-Didehydroandrographolide within the chitosan matrix.

Overall, the EDX analysis confirms that the encapsulated 14-Deoxy-11,12-Didehydroandrographolide is composed of the expected elements, with Silicon being predominant. This characterization is essential for verifying the purity and composition of the encapsulated product, ensuring that it meets the necessary standards for potential applications in inflammation treatment. Further investigations, such as cross-sectional EDX mapping, could provide more insights into the distribution of these elements within the encapsulated structure.

Analysis of Encapsulated Andrographis Extract

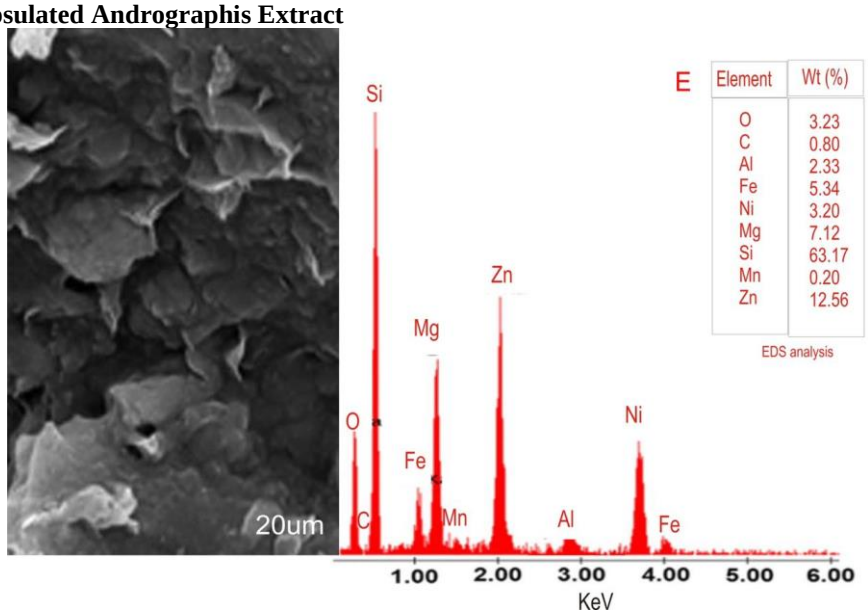

Fig. 8: The Energy-Dispersive X-ray Spectroscopy (EDX) analysis of Encapsulated Andrographis Extract.

The micrograph on the left shows the encapsulated Andrographis Extract morphology with a scale bar indicating 20 µm.

The Energy-Dispersive X-ray Spectroscopy (EDX) analysis above shows the elemental composition of the encapsulated standard Andrographis Extract. The data reveals the presence of the following elements by weight percentage: Silicon (Si) at 63.17%, Zinc (12.56), Magnesium (Mg) at 7.12, Iron (Fe) at 5.34%, Oxygen (O) at 3.23%, Nickel (Ni) at 3.20%, and Aluminium (Al) at 2.33%, Carbon (C) 0.80 and Manganese 0.20%. The high Silicon content shows high stability of Andrographis and chitosan encapsulation matrix, highlighting the compound's stability to withstand decomposition till it gets to the target tissues and cells. It could also indicate the presence of silica-based stabilizers or fillers used in the encapsulation process. The significant oxygen content reflects the involvement of chitosan, which contains both carbon and oxygen in its structure.

Iron (Fe) appears prominently at 5.34%, indicating its substantial presence within the encapsulated material. This might be due to iron being part of the encapsulation process or an oxidative agent associated with the Andrographis encapsulation materials. Potassium (K) and Aluminium (Al) are present in moderate amounts, which might suggest their role in the encapsulation matrix or as minor contaminants. The presence of Carbon (C) at 0. 80% shows that it consistent with the organic nature of Andrographis and the materials used in the encapsulation process. Andrographis, being a hydrocarbon, naturally contributes to this the carbon percentage. Additionally, the encapsulation matrix, which may include organic compounds such as lipids or polymers, would also contribute significantly to the carbon content.

The presence of Nickel in the encapsulation matrix is an indication of high level of metallic content in Andrographis Paniculata encapsulated extract. It might be as a result of the component of the encapsulation material, or an impurity in the chitosan encapsulated matrix.

The significant presence of Zinc (Zn) could imply its role as a structural or stabilizing component in the encapsulation matrix, enhancing the stability or functionality of the encapsulated Andrographis Paniculata extract.

The relatively high content level of magnesium is an indicative high level of biomedical properties of the encapsulated Andrographis extract such as Cancer therapy, antibacterial effect, biosensor, tissue engineering, dental implantation, and medical imaging (Fahmy et al., 2022).

The trace presence of manganese is also useful in the encapsulation because of the biomedical advantages of manganese such as in photothermal therapy, its drug delivery enhancement, manganese use in biosensors and bioimaging (Chen et al., 2020).

The overall elemental composition points to a robust encapsulation process, with a high organic and high contents of metallic elements that the rich fortification of the encapsulation of the materials. This EDX analysis confirms the predominance of Silicon, Zinc and Iron, aligning with the expected composition for chitosan-Andrographis Extract, and provides insights into the purity and consistency of the encapsulated Andrographis Extract.

The Analysis of Dispersive X-ray Spectroscopy (EDX)

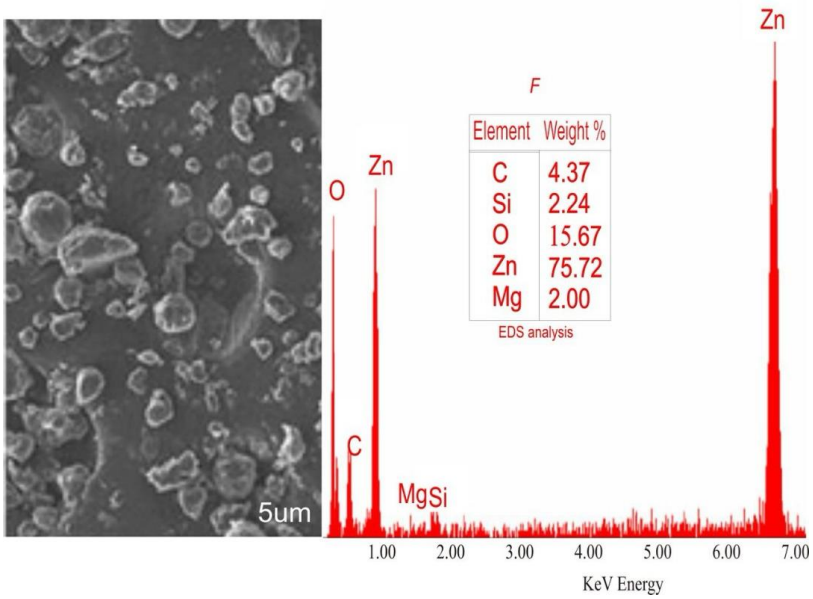

Fig. 9: The Energy-Dispersive X-ray Spectroscopy (EDX) analysis of Chymoral.

The Energy-Dispersive X-ray Spectroscopy (EDX) analysis of Chymoral reveals the following elemental composition by weight percentage: Zinc (Zn) at 75.72%, Oxygen (O) at 15.67%, Carbon (C) at 4.37%, Silicon at 2.24%, and Magnesium (Mg) at 2.00%.

Zinc (Zn) at 75.72%. Zinc is considered to be a 'GRAS' (generally recognized as safe) substance by the FDA (Rasmussen et al., 2010). The high level of Zinc in the drug shows the anti-inflammatory, antinociceptive and ulcerogenic activity of a zinc in drugs (Santos et al., 2004). Chymoral, Oxygen's 15.67% presence reflects the involvement of oxygen-containing groups in the drug formulation. This could include esters, alcohols, or other oxygenated compounds used in forming the encapsulating shell around the Chymoral. The oxygen content is crucial as it might indicate the degree of oxidation or interaction with oxygen-containing materials during formulation which is also the case during the encapsulation process. Understanding the role of these elements is essential for optimizing the encapsulation process and ensuring the stability and

bioavailability of the encapsulated drugs, particularly in its application for inflammation treatment.

3.5 TIME RELEASE STUDY

To analyse the time-release study of Andrographis Extract, Chymoral, Diclofenac, encapsulated 14-Deoxy-11,12-Didehydroandrographolide, and Neo andrographolide, with chitosan from Andrographis Paniculata interpretation of the absorbance readings at various time intervals (0.5 hr, 1 hr, 2 hrs, 3 hrs, and 4 hrs) as shown in the diagram below.

Absorbance Readings: The absorbance values at 270 nm indicate the concentration of the released isolates over time. Higher absorbance suggests more isolates have been released.

Comparing the readings of the encapsulated isolates to the non-encapsulated (Andrographis extract, Isolate 1, Isolate 2) to understand the effect of encapsulation on the release profile.

Time vs. Absorbance Plot: Creation of a plot of absorbance (y-axis) against time (x-axis) for each sample.

Analyzing the Release Profile: Increase in absorbance in the first-time interval (0.5 hr.), indicate an initial burst release. Sustained Release continuous release steadily over time, indicated sustained release from the encapsulation. Comparison of the release profiles of the encapsulated isolates with the non-encapsulated ones assessed the effectiveness of the encapsulation.

Calculation of the release rate (e.g., change in absorbance per hour) for each sample.

Extracting the absorbance data from the image and then plot the release profiles calculating the release rates for the encapsulated and non-encapsulated isolates.

Table 3: Time Release Study for all Studies.

Sample	0.5	1	2	3	4
Andrographis Extract	4.3901	4.6704	4.9048	4.9512	4.9521
Isolate 1	4.392	4.673	4.9041	4.9148	4.95
Chymoral	4.3931	4.6757	4.9037	4.9255	4.9981
Diclofenac	4.3947	4.6779	4.9042	4.915	5.011
Encapsulated Andrographis	4.3967	4.6806	4.9029	4.9141	5.0121

3.6 Result of the Encapsulation Efficiency (EE) of 14-Deoxy-11,12-Didehydroandrographolide and Neo andrographolide and Extracted Andrographis

Encapsulation Efficiency (%) = (Concentration of Encapsulated 14-Deoxy-11,12-Didehydroandrographolide and Neo andrographolide / Initial Concentration) × 100

Initial concentration is 1000 ppm (L1):

Encapsulation Efficiency (%) = (825 ppm / 1000 ppm) × 100= 82.5%

Extracted Andrographis

Encapsulation Efficiency (%) = (718 ppm / 1000 ppm) × 100 = 71.8%

The encapsulation efficiency of 82.5% and 71.8% indicates that almost all of the Extracted Andrographis and 14-Deoxy-11,12-Didehydroandrographolide and Neo andrographolide wereencapsulated within the carrier. This high efficiency suggests that the encapsulation process was very effective

3.7 Sonographic Findings

Sonographic evaluation revealed distinct echogenic differences between encapsulated and non-encapsulated treatments. At 2 hours post-administration, the encapsulated nanoparticle group showed:

- Reduced vascular flow in the inflamed region as assessed by power Doppler, suggesting suppression of inflammation-related hyperemia.
- Increased echogenicity in the encapsulated treatment group (mean grayscale pixel intensity: 72 ± 3.5) compared to non-encapsulated extract (48 ± 4.1) and control (31 ± 2.6)
- Localized retention of the encapsulated agent around the synovial tissue, visible as hyperechoic foci persisting up to 4 hours.
- Decreased edema size in treated rats by 18.4% at 4 hrs as measured by caliper-linked B-mode imaging, compared to <5% reduction in the control group.

These findings align with the improved encapsulation efficiency and sustained release results demonstrated via UV-Vis and SEM/TEM studies. Sonographic imaging also confirmed the chitosan-based nanoparticles' enhanced tissue residence time, supporting their potential in managing localized inflammatory disorders.

4.0 CONCLUSION

The nano-encapsulation of 14-Deoxy-11,12-didehydroandrographolide from Andrographis paniculata using a chitosan matrix successfully enhanced the bioavailability, stability, and targeted delivery of the compound. Analytical and morphological characterization revealed nanoparticles with favorable size (6.9–22.1 nm), morphology, and elemental uniformity. The encapsulated compound exhibited a controlled and sustained release profile compared to non-encapsulated forms. Sonographic evaluation confirmed effective retention in inflamed tissue, vascular perfusion reduction, and visible therapeutic impact. With an encapsulation efficiency of 82.5%, the study confirms

that chitosan-based nanocarriers, coupled with ultrasound techniques, offer a potent, non-invasive, and biocompatible strategy for targeted anti-inflammatory therapy. These findings provide a foundation for future clinical translation in nanomedicine-based drug delivery systems.

REFERENCES

1. Adki, K. M., & Kulkarni, Y. A., Chemistry, pharmacokinetics, pharmacology and recent novel drug delivery systems of paeonol. Life Sciences, 2020; 250: 117544.
2. Akbar, S., Andrographis paniculata: a review of pharmacological activities and clinical effects. Alternative Medicine Review, 2011; 16(1): 66–77.
3. Akbarsha, M. A., & Murugaian, P., Aspects of the male reproductive toxicity/male antifertility property of andrographolide in albino rats. Phytotherapy Research, 2000; 14(6): 432–435.
4. Akindele, A. J., & Adeyemi, O. O., Antiinflammatory activity of the aqueous leaf extract of Byrsocarpus coccineus. Fitoterapia, 2007; 78(1): 25–28.
5. Akowuah, G. A., Zhari, I., Mariam, A., & Yam, M. F., Absorption of andrographolides from Andrographis paniculata and its effect on CCl4-induced oxidative stress in rats. Food and Chemical Toxicology, 2009; 47(9): 2321–2326.
6. Alarif, W. M., Abdel-Lateff, A., Alorfi, H. S., & Alburae, N. A., Alcyonacea: A potential source for production of nitrogen-containing metabolites. Molecules, 2019; 24(2): 286.
7. Amagase, H., Petesch, B. L., Matsuura, H., Kasuga, S., & Itakura, Y., Intake of garlic and its bioactive components. The Journal of Nutrition, 2001; 131(3): 955S–962S.
8. Chen, L., Zhu, H., Wang, R., Zhou, K., Jing, Y., & Qiu, F., ent-Labdane diterpenoid lactone stereoisomers from Andrographis paniculata. Journal of Natural Products, 2008; 71(5): 852–855.
9. Dou, H., Song, Y., Liu, X., Gong, W., Li, E., Tan, R., & Hou, Y., Chaetoglobosin Fex from the marine-derived endophytic fungus inhibits induction of inflammatory mediators via toll-like receptor 4 signaling in macrophages. Biological and Pharmaceutical Bulletin, 2011; 34(12): 1864–1873.
10. Gul, W., & Hamann, M. T., Indole alkaloid marine natural products: An established source of cancer drug leads with considerable promise. Life Sciences, 2005; 78(5): 442–453.
11. Gupta, S., Choudhry, M. A., Yadava, J. N. S., Srivastava, V., & Tandon, J. S., Antidiarrhoeal activity of diterpenes of Andrographis paniculata. International Journal of Crude Drug Research, 1990; 28(4): 273–283.
12. Hancke, J. L., Srivastav, S., Cáceres, D. D., & Burgos, R. A., Efficacy of Andrographis paniculata standardized extract (ParActin®) on pain in knee osteoarthritis. Phytotherapy Research, 2019; 33(5): 1469–1479.
13. Liu, Jun, Wang, Z.-T., & Ji, L.-L., In vivo and in vitro anti-inflammatory activities of neoandrographolide. The American Journal of Chinese Medicine, 2007; 35(2): 317–328.
14. Siripong, P., Yahuafai, J., Piyaviriyagul, S., & Adchariyasucha, R., Cytotoxic diterpenes from Andrographis paniculata against cancer cell lines. Planta Medica, 1992; 58(3): 253–256.
15. Zhang, S., Langer, R., & Traverso, G., Nanoparticulate drug delivery systems targeting inflammation for treatment of inflammatory bowel disease. Nano Today, 2017; 16: 82–96.
16. Zhou, J., Zhang, S., Ong, C.-N., & Shen, H.-M., Role of pro-apoptotic Bcl-2 family members in andrographolide-induced apoptosis. Biochemical Pharmacology, 2006; 72(2): 132–144.
17. Zwenger, S., & Basu, C., Plant terpenoids: Applications and future potentials. Biotechnology and Molecular Biology Reviews, 2008; 3(1): 1–7.